

**Weibull model of multiplicity distribution in hadron-hadron collisions**Sadhana Dash,<sup>\*</sup> Basanta K. Nandi, and Priyanka Sett*Indian Institute of Technology, Bombay 400076, India*

(Received 15 January 2016; revised manuscript received 1 June 2016; published 20 June 2016)

We introduce the use of the Weibull distribution as a simple parametrization of charged particle multiplicities in hadron-hadron collisions at all available energies, ranging from ISR energies to the most recent LHC energies. In statistics, the Weibull distribution has wide applicability in natural processes that involve fragmentation processes. This provides a natural connection to the available state-of-the-art models for multiparticle production in hadron-hadron collisions, which involve QCD parton fragmentation and hadronization. The Weibull distribution describes the multiplicity data at the most recent LHC energies better than the single negative binomial distribution.

DOI: [10.1103/PhysRevD.93.114022](https://doi.org/10.1103/PhysRevD.93.114022)**I. INTRODUCTION**

Inclusive charged particle multiplicity distribution had been extensively studied in hadronic collisions. The multiplicity distribution characterizes the hadronic final state and provides important insights on the production mechanism of multiparticle final states. In particular, they are sensitive to the underlying quantum chromodynamics (QCD) in hadron-hadron collisions. The previous phenomenological studies of multiplicity distributions at various energies have been done in terms of parameters of the negative binomial distribution (NBD) function. Although the interpretation of the NBD function in terms of particle production is not fully understood, it remarkably described the data at lower energies [1]. However, deviations from the NBD function were observed at higher energies [1–3], which puts constraints on its universal applicability for a wider range of energies. The use of single NBD function was followed by the two-component model of particle production, where one component was interpreted to be soft and the other as semihard [4]. This led to the description of the data by the weighted combination of two NBD functions. The multiplicity distributions at LHC energies and for all pseudorapidity intervals were well described by this approach [2,5]. However, it was pointed out that the excellent description of multiplicity distributions of hard QCD events in forward rapidity of  $pp$  collisions at 7 TeV contradicts the very concept of the two-component model [5]. The framework of a weighted superposition of distributions to explain various classes of events has also been extended to the three-component model in order to explain the multiplicity distributions at LHC energies for  $pp$  collisions at 14 TeV [6]. Recently, models based on glasma flux tubes have reproduced the multiplicity distribution in  $pp$  collisions at LHC energies in midrapidity using the superposition of many NBD functions [7].

However, one should note that with the superposition of two or more NBD functions, one increases the number of free parameters in the resultant function and, hence, fitting the experimental distribution becomes mathematically easier. A detailed discussion on multiplicity measurements and various approaches can be found in [8].

In this work, we introduce a statistical distribution—namely, the Weibull distribution [9] based on an appealing physical interpretation. Our objective is to provide a single two-parameter function that can broadly describe the principal feature of the multiplicity distribution for most of the available experimental measurements in  $pp(p\bar{p})$  systems at all available energies from intersecting storage rings (ISR) to LHC.

**II. WEIBULL DISTRIBUTION**

Many evolving systems in nature exhibit skewed distributions; among them, Weibull and log-normal distributions commonly appear in a variety of systems [9,10]. In particular, the Weibull-like distribution is widely used to describe size distribution obtained in diverse fields such as material fragmentation [11], cloud droplets [12], biological systems [13,14], wind speeds [15], extreme-value statistics [16,17], and so forth. Since final-state particle multiplicity can be seen as having evolved from initial hadron-hadron collisions, one can expect to use the Weibull-like distribution to describe the probability of producing charged particles.

The probability distribution of a continuous random variable  $n$  in terms of a two-parameter Weibull distribution is given by

$$P(n, \lambda, k) = \frac{k}{\lambda} \left(\frac{n}{\lambda}\right)^{k-1} e^{-(n/\lambda)^k}, \quad (1)$$

where  $k$  is the shape parameter and  $\lambda$  is the scale parameter of the distribution. The mean of the distribution is given in terms of  $\lambda$  and  $k$  as

---

<sup>\*</sup>sadhana@phy.iitb.ac.in

$$\langle n \rangle = \lambda \Gamma \left( 1 + \frac{1}{k} \right). \quad (2)$$

The description of a physically based derivation of the Weibull distribution with respect to fragmentation processes can be found in [11]. In Ref. [11], it was shown that the result of a single event fragmentation leading to a branching tree of cracks in the material that show fractal behavior can be described by a Weibull-like distribution. This can be related to the mass distribution or particle number distribution developed by the fragmentation process. It was also shown that a particular mass distribution closely resembles the log-normal distribution, which has been commonly used for describing fragmentation distributions [11]. The log-normal distribution also described well the particle multiplicities at ISR energies [18].

The underlying mechanism of particle production in hadronic collisions as given by current models is based on the fragmentation of partons into observed hadrons. Irrespective of particular details, most of the models of multiparticle production contain an evolution composed of various steps that are based on previous intermediate steps and are influenced by the same. The steps involving hard and semihard processes are well explained by perturbative QCD [19–21], whereas models for soft interactions involve a large class of string fragmentation models [22,23]. The cascade nature of models involving fragmentation of partons is apparent and, thus, one can use the Weibull distribution to model the basic multiplicity distribution in hadron-hadron collisions. This also corroborates to the clan model that involves particle cascades as a mechanism of particle production [2,4].

Because the multiplicity in a collision is a result of the fragmentation of the energy (invariant mass of initial partons) involved in the initial scattering into masses (or packets of energy), we are more interested in the distribution of this fragmented energy or mass. Alternatively, one can use the weight-size distribution in the fragmentation of bulk matter, resulting in macroscopic mass distribution [11]. If  $n(\epsilon)$  describes the number of particles produced with fragmented energy (or mass) between  $\epsilon$  and  $\epsilon + d\epsilon$ , and each of the particles has an energy  $\epsilon$ , then the energy distribution is simply  $\epsilon n(\epsilon)$ . Its distribution follows [11]

$$\epsilon n(\epsilon) = \frac{k}{\lambda} \left( \frac{\epsilon}{\lambda} \right)^{k-1} e^{-(\epsilon/\lambda)^k}. \quad (3)$$

The above distribution is a Weibull distribution in energy, where the  $\lambda$  parameter is related to the average value of the fragmented energy (and can be related to the mean multiplicity) in the collision, while the value of  $k$  parameter is associated to the dynamics of the fragmentation process. We can relate the distribution of the number of particles produced in a collision as the distribution of fragments of initial energy and, thus, can effectively use the

Weibull distribution to describe the multiplicity in hadron-hadron collisions.

### III. MULTIPLICITY DISTRIBUTION AND WEIBULL PARAMETERS

In the present scenario, where we have experimental data on multiplicity distributions in widest range of energies and pseudorapidity intervals, it is worth trying to determine whether one can parametrize the data in terms of Weibull parameters. We identify the variable  $n$  with the charged particle multiplicity and perform fits to the data points using the chi-square minimization method.

The multiplicity distributions were fitted with a Weibull function in  $p\bar{p}$  and  $pp$  collisions as measured by the UA5 experiment at super proton synchrotron energies [1] and by CMS experiments [24] at LHC energies, respectively. Figure 1 shows the Weibull fits to the multiplicity distribution at  $|\eta| < 0.5$  for the  $p\bar{p}$  collisions as measured by UA5 experiment at 200 GeV, 540 GeV, and 900 GeV center-of-mass energies. The Weibull fits to the multiplicity distribution in  $pp$  collisions at  $|\eta| < 0.5$  as measured by CMS experiment at various energies are depicted in Fig. 2.

Table I lists all the parameters obtained from the Weibull fits together with  $\chi^2/\text{NDF}$  and extracted mean multiplicity for different collision systems studied.

The multiplicity distributions measured by the CMS experiment at three LHC energies, i.e., 0.9 TeV, 2.36 TeV, and 7 TeV, for wider pseudorapidity intervals and for the same class (non-single-diffractive class) were also analyzed. The multiplicity distribution was earlier analyzed with a single NBD distribution; this resulted in poor

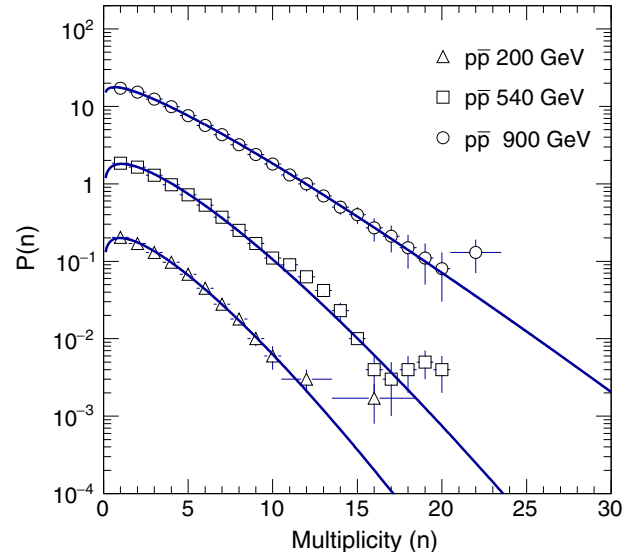


FIG. 1. UA5 measurement of charged particle multiplicity distributions in  $p\bar{p}$  collisions for  $|\eta| < 0.5$  at  $\sqrt{s} = 200$  GeV, 540 GeV, and 900 GeV [1]. The solid lines represent the Weibull fits to the data points. The data points for a given energy are appropriately scaled for better visibility.

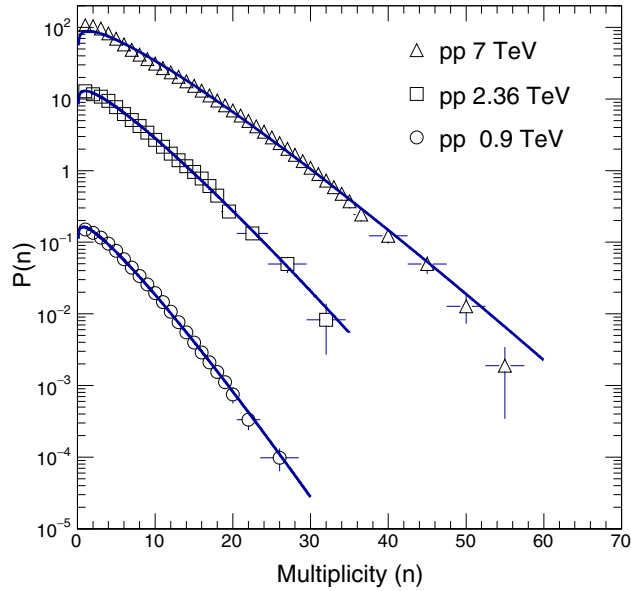


FIG. 2. CMS measurement of charged particle multiplicity in  $pp$  collisions for  $|\eta| < 0.5$  at  $\sqrt{s} = 0.9$  TeV, 2.36 TeV, and 7 TeV [24]. The solid lines represent the Weibull fits to the data points. The data points for a given energy are appropriately scaled for better visibility.

agreement with the data, specifically in wider pseudorapidity intervals. It was followed by a description with a weighted superposition of two NBD functions, which described the data successfully [2]. However, we are not comparing the Weibull distribution with the double NBD function, as the number of parameters in the latter is higher. We are also not discussing two- (or more) component particle production in the Weibull parametrization. We want to emphasize that a single distribution is able to describe the global feature of the particle production. The fits to the recent multiplicity distributions in  $pp$  collisions as measured by the CMS experiment at various energies (for different  $\eta$  intervals) are shown in Figs. 3, 4, and 5, respectively. The fits from the single NBD function are also shown for comparison. As can be seen from the figures, the Weibull fits give a better description of the data at all energies and at all pseudorapidity intervals compared

TABLE I. List of parameters and  $\chi^2/\text{NDF}$  values of the Weibull fits to the data for various collision systems at different energies for  $|\eta| < 0.5$ .

Collision systems	$\sqrt{s}$ (TeV)	$k$	$\lambda$	$\chi^2/\text{NDF}$	$\langle n \rangle$
$p\bar{p}$	0.2	$1.27 \pm 0.04$	$3.17 \pm 0.17$	0.54	$2.93 \pm 0.29$
$p\bar{p}$	0.54	$1.26 \pm 0.01$	$3.58 \pm 0.14$	1.66	$3.32 \pm 0.15$
$p\bar{p}$	0.9	$1.11 \pm 0.01$	$4.07 \pm 0.18$	0.33	$3.91 \pm 0.15$
$pp$	0.9	$1.18 \pm 0.03$	$4.17 \pm 0.16$	0.03	$3.98 \pm 0.18$
$pp$	2.36	$1.14 \pm 0.03$	$5.41 \pm 0.15$	0.22	$5.15 \pm 0.36$
$pp$	7	$1.15 \pm 0.01$	$7.35 \pm 0.16$	0.85	$6.98 \pm 0.26$

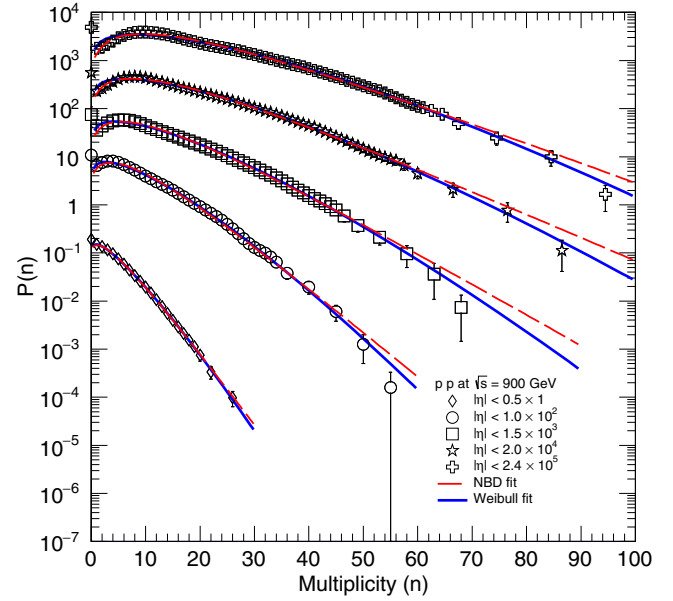


FIG. 3. CMS measurement [24] of charged particle multiplicity distributions in  $pp$  collisions for different pseudorapidity intervals at  $\sqrt{s} = 0.9$  TeV. The solid lines represent the Weibull fits to the data points while the dashed lines represent the standard single NBD fits. The data points for a given pseudorapidity interval are appropriately scaled for better visibility.

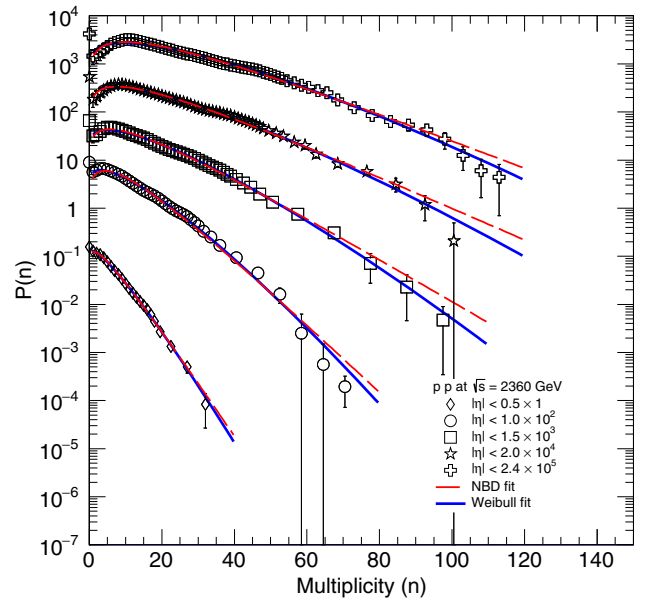


FIG. 4. CMS measurement [24] of charged particle multiplicity distributions in  $pp$  collisions for different pseudorapidity intervals at  $\sqrt{s} = 2.36$  TeV. The solid lines represent the Weibull fits to the data points while the dashed lines represent the standard single NBD fits. The data points for a given pseudorapidity interval are appropriately scaled for better visibility.

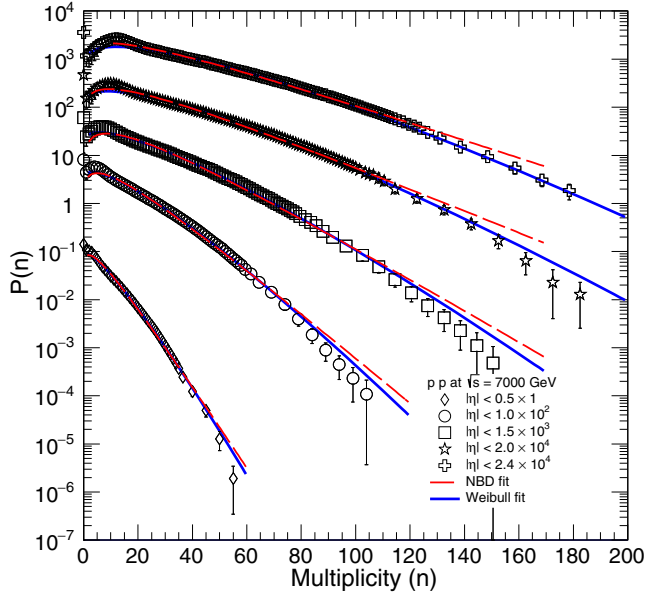


FIG. 5. CMS measurement [24] of charged particle multiplicity distributions in  $pp$  collisions for different pseudorapidity intervals at  $\sqrt{s} = 7.0$  TeV. The solid lines represent the Weibull fits to the data points while the dashed lines represent the standard single NBD fits. The data points for a given pseudorapidity interval are appropriately scaled for better visibility.

to the single NBD function. The values of the parameters and the  $\chi^2/\text{NDF}$  of the fit are tabulated in Tables II, III, and IV.

At LHC energies, the multiplicity distribution as measured by LHCb experiment covers the widest range of

TABLE II. List of parameters and  $\chi^2/\text{NDF}$  values of the Weibull fits to the data at  $\sqrt{s} = 900$  GeV for different pseudorapidity intervals.

$\eta$ interval	$k$	$\lambda$	$\chi^2/\text{NDF}$	$\langle n \rangle$
-0.5-0.5	$1.18 \pm 0.03$	$4.17 \pm 0.16$	0.035	$4.14 \pm 0.09$
-1.0-1.0	$1.28 \pm 0.02$	$8.60 \pm 0.17$	0.362	$7.97 \pm 0.13$
-1.5-1.5	$1.31 \pm 0.02$	$12.70 \pm 0.17$	0.333	$11.71 \pm 0.16$
-2.0-2.0	$1.34 \pm 0.02$	$16.88 \pm 0.23$	0.332	$15.50 \pm 0.18$
-2.4-2.4	$1.38 \pm 0.02$	$20.33 \pm 0.26$	0.444	$18.57 \pm 0.20$

TABLE III. List of parameters and  $\chi^2/\text{NDF}$  values of the Weibull fits to the data at  $\sqrt{s} = 2.36$  TeV for different pseudorapidity intervals.

$\eta$ interval	$k$	$\lambda$	$\chi^2/\text{NDF}$	$\langle n \rangle$
-0.5-0.5	$1.14 \pm 0.03$	$5.41 \pm 0.16$	0.22	$5.16 \pm 0.11$
-1.0-1.0	$1.25 \pm 0.02$	$10.86 \pm 0.22$	0.69	$10.11 \pm 0.17$
-1.5-1.5	$1.27 \pm 0.02$	$16.23 \pm 0.19$	0.37	$15.07 \pm 0.13$
-2.0-2.0	$1.29 \pm 0.03$	$21.54 \pm 0.25$	0.53	$19.92 \pm 0.14$
-2.4-2.4	$1.33 \pm 0.02$	$25.96 \pm 0.28$	0.54	$23.87 \pm 0.19$

TABLE IV. List of parameters and  $\chi^2/\text{NDF}$  values of the Weibull fits to the data at  $\sqrt{s} = 7.0$  TeV for different pseudorapidity intervals.

$\eta$ interval	$k$	$\lambda$	$\chi^2/\text{NDF}$	$\langle n \rangle$
-0.5-0.5	$1.15 \pm 0.015$	$7.35 \pm 0.15$	1.13	$6.99 \pm 0.12$
-1.0-1.0	$1.20 \pm 0.013$	$14.56 \pm 0.23$	1.02	$13.69 \pm 0.18$
-1.5-1.5	$1.23 \pm 0.011$	$21.89 \pm 0.29$	1.08	$20.45 \pm 0.22$
-2.0-2.0	$1.27 \pm 0.011$	$30.02 \pm 0.16$	1.09	$27.85 \pm 0.09$
-2.4-2.4	$1.30 \pm 0.017$	$36.44 \pm 0.18$	1.25	$33.65 \pm 0.06$

pseudorapidity intervals in  $pp$  collisions at 7 TeV [25]. The LHCb experiment has measured multiplicity distributions of charged particles produced for two classes of events: the minimum bias and the hard QCD events. The hard QCD events were selected from the minimum bias events by identifying events with at least one particle with transverse momentum greater than 1 GeV/c. The distributions were analyzed for both the event classes in forward rapidity ( $2.0 < \eta < 4.5$ ) using the Weibull function. The single NBD distribution could not give a good description of the data in the forward rapidity for both the event classes [5]. Figure 6 shows the Weibull fits to the LHCb data in forward rapidity ( $2.0 < \eta < 4.5$ ) for both the event classes. The data is nicely described by the Weibull distribution for minimum bias and the hard QCD events. The applicability was also checked at lower energies measured by the ISR experiment [26], as shown in Fig. 7. This figure provides an excellent

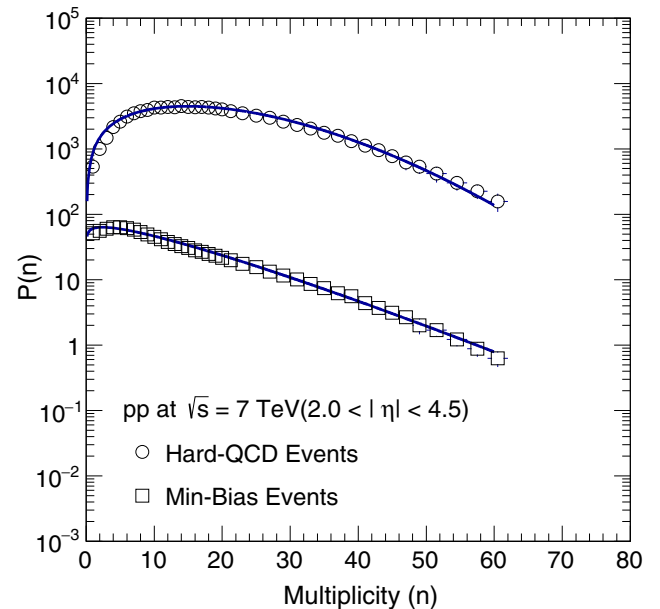


FIG. 6. LHCb measurement [20] of charged particle multiplicity distributions in  $pp$  collisions for two different event classes in forward rapidity ( $2.0 < \eta < 4$ ) regions at  $\sqrt{s} = 7$  TeV. The solid lines represent the Weibull fits to the data points. The data points for a given energy are appropriately scaled for better visibility.

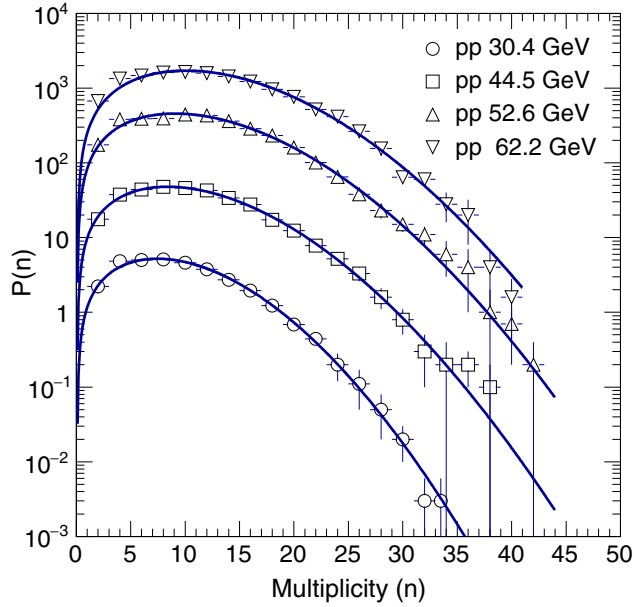


FIG. 7. ISR measurement of topological cross sections as a function of multiplicity in  $pp$  collisions (for  $|\eta| < 4.0$ ) at various center-of-mass energies [21]. The solid lines represent the Weibull fits to the data points. The data points for a given energy are appropriately scaled for better visibility.

comparison, in which we observe that the Weibull distribution successfully explains the data at two diverse energy regimes.

The energy dependence of the mean charged multiplicity reflects the underlying particle production mechanism. Feynman scaling predicts that the total mean number of

particles produced obeys an energy dependence proportional to  $\ln(\sqrt{s})$  [27]. Figure 8 shows the mean multiplicity as a function of the center-of-mass energy. As can be observed from the figure, the mean multiplicity increases with an increase of collision energy, and the variation of mean multiplicity with beam energy can be quantified by the expression

$$\langle n \rangle = \mathbf{A} + \mathbf{B} \ln(\sqrt{s}) + \mathbf{C} \ln^2(\sqrt{s}). \quad (4)$$

We also observe that the scale parameter,  $\lambda$ , shows an energy dependence similar to that of the mean multiplicity. This is shown in Fig. 9. The observed variation of the  $\lambda$  parameter is expected, as  $\lambda$  is related to mean multiplicity. Figure 10 shows the variation of  $\lambda$  as a function of  $\eta$  for various LHC energies. The value of  $\lambda$  increases with increasing  $\eta$  intervals and energy. The observed behavior is expected, as the number of particles produced increases with increase in collision energy and  $\eta$  intervals.

It can be seen from Table I that the values of the shape parameter  $k$  do not vary significantly with the center-of-mass energy. However, there is a slight decrease in the  $k$  value with an increase in collision energy. This is also shown in Fig. 11 for different  $\eta$  intervals for different available LHC energies. It should be also noted that the  $k$  value has an increasing trend with an increase in  $\eta$  intervals. One can interpret that the  $k$  value becomes higher with an enhanced contribution of particle production from soft processes. As the  $k$  parameter is related to the nature of the fragmentation process, one can say that the dynamics associated with the fragmentation process in hadron-hadron

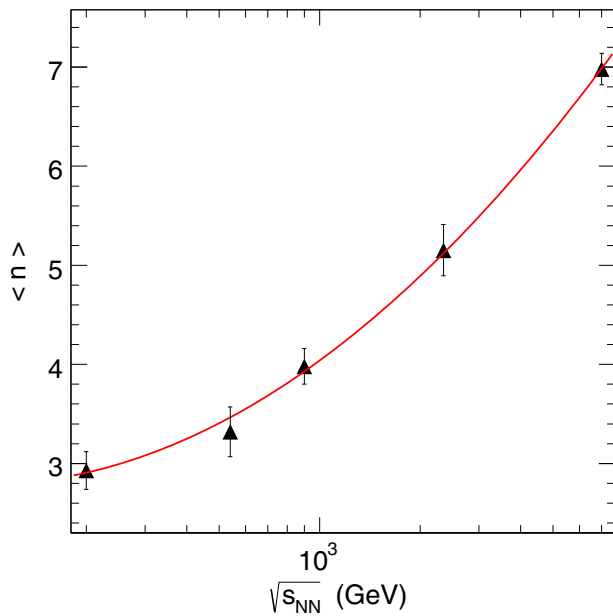


FIG. 8. The variation of mean multiplicity for  $|\eta| < 0.5$  as a function of center-of-mass energy. The solid line represents the fit given by expression (4) to the data points.

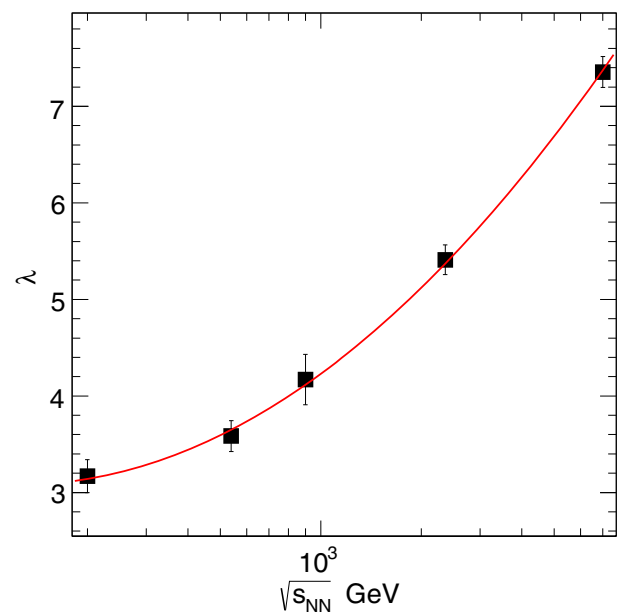


FIG. 9. The variation of the  $\lambda$  parameter extracted from the Weibull fit as a function of beam energy. The solid line represents the fit given by expression (4) to the data points.

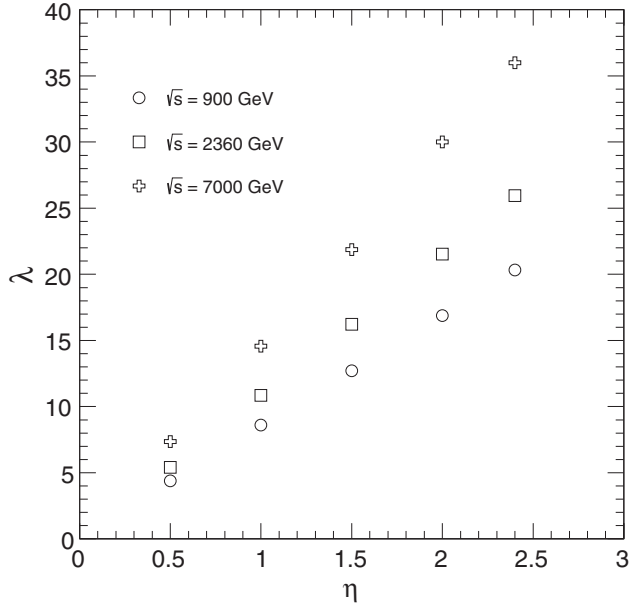


FIG. 10. The variation of the  $\lambda$  parameter as a function of  $\eta$  for various energies.

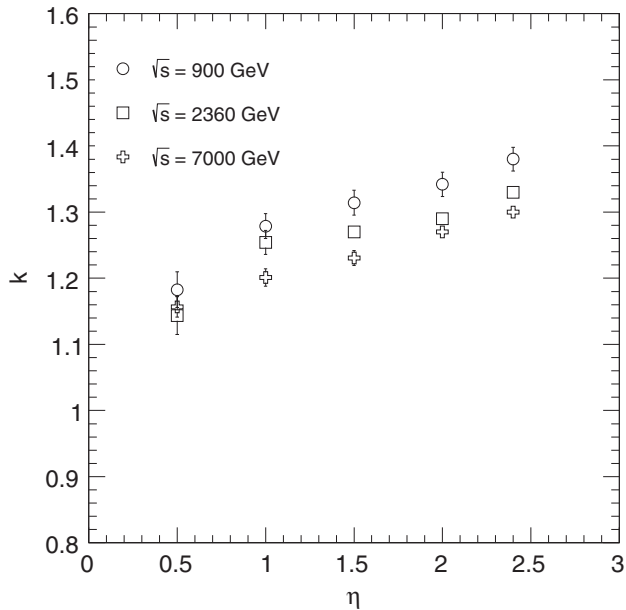


FIG. 11. The variation of the  $k$  parameter as a function of  $\eta$  for various energies.

collisions do not vary significantly with the center-of-mass energy in similar  $\eta$  intervals.

Taking this into account, as well as the extrapolated values of the  $\lambda$  parameter, we predict the multiplicity distributions in  $pp$  collisions at the recent LHC run at 13.0 TeV ( $\lambda = 8.75 \pm 2.78$ ,  $k = 1.15 \pm 0.012$ ). Figure 12

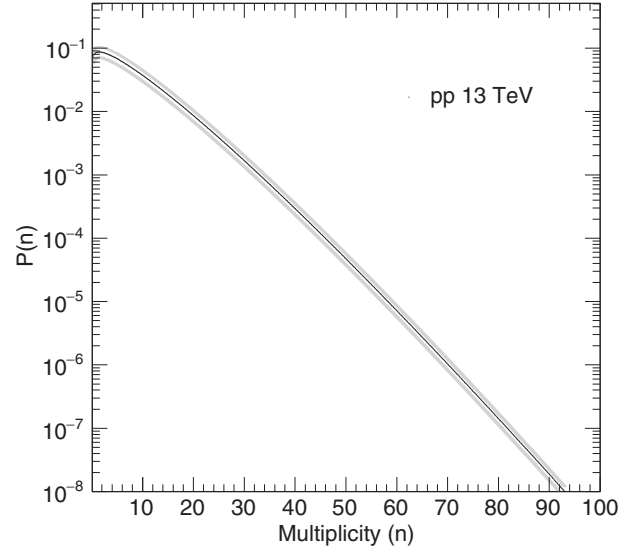


FIG. 12. The charged particle multiplicity distribution in  $pp$  collisions for  $|\eta| < 0.5$  at  $\sqrt{s} = 13.0$  TeV as predicted by Weibull parametrization. The shaded band around the solid line shows the associated systematic errors.

depicts the predicted multiplicity distributions at  $\sqrt{s} = 13.0$  TeV for  $|\eta| < 0.5$ . The shaded band on the data points shows a systematic error band that is due to various sources including variation in fitting parameters, ranges, and so forth. The mean multiplicity,  $\langle n \rangle$ , at 13.0 TeV turns out to be  $8.30 \pm 2.96$ . The measurement of multiplicity distributions at larger  $\sqrt{s}$  at LHC will be a first test of the further applicability of the Weibull distribution and will add credibility to the extrapolation.

#### IV. SUMMARY

We have demonstrated that the Weibull distribution provides an excellent description of the multiplicity distributions of inclusive charged particles in hadronic collisions at all available energies and at all pseudorapidity intervals. This is particularly significant because the Weibull distribution arises in cascade processes that involve the fragmentation of the source. This leads to a very interesting physics interpretation in terms of current dynamical models of multiparticle production. The  $\lambda$  parameter can be related to mean multiplicity. The  $k$  parameter does not vary significantly with energy in similar pseudorapidity intervals, indicating the universal nature of parton fragmentation and subsequent hadronization. We observe that the Weibull distribution provides more appropriate descriptions of multiplicity distributions compared to the existing statistical functions used in multiparticle production processes.

- [1] R. E. Ansorge *et al.* (UA5 Collaboration), *Z. Phys. C* **43**, 357 (1989).
- [2] P. Ghosh, *Phys. Rev. D* **85**, 054017 (2012).
- [3] F. Rimondi *et al.* (CDF Collaboration), in *Proceedings of the XXIII International Symposium on Multiparticle Dynamics, Aspen, Colorado, USA, 12–17 September 1993* (World Scientific, Singapore, 1994), p. 400.
- [4] A. Giovannini and R. Ugoccioni, *Phys. Rev. D* **60**, 074027 (1999).
- [5] P. Ghosh and S. Muhuri, *Phys. Rev. D* **87**, 094020 (2013).
- [6] A. Giovannini and R. Ugoccioni, *Phys. Rev. D* **68**, 034009 (2003).
- [7] P. Tribedy and R. Venugopalan, *Nucl. Phys. A* **850**, 136 (2011).
- [8] J. F. Grosse-Oetringhaus and K. Reygiers, *J. Phys. G* **37**, 083001 (2010).
- [9] W. Weibull, *J. Appl. Mech.* **18**, 293 (1951).
- [10] M. Y. Choi, H. Choi, J. Y. Fortin, and J. Choi, *Europhys. Lett.* **85**, 30006 (2009).
- [11] W. K. Brown and K. H. Wohletz, *J. Appl. Phys.* **78**, 2758 (1995).
- [12] Y. Liu and J. Hallett, *J. Atmos. Sci.* **55**, 527 (1998).
- [13] J. Jo, M. Y. Choi, and D. S. Koh, *Biophys. J.* **93**, 2655 (2007).
- [14] J. Jo, J. Y. Fortin, and M. Y. Choi, *Phys. Rev. E* **83**, 031123 (2011).
- [15] E. S. Takle and J. M. Brown, *J. Appl. Meteorol.* **17**, 556 (1978).
- [16] E. Bertin and M. Clusel, *J. Phys. A* **39**, 7607 (2006).
- [17] N. R. Moloney and J. Davidsen, *Phys. Rev. E* **79**, 041131 (2009).
- [18] S. Carius and G. Ingelman, *Phys. Lett. B* **252**, 647-652 (1990).
- [19] T. K. Gaisser, F. Halzen, A. D. Martin, and C. J. Maxwell, *Phys. Lett.* **166B**, 219 (1986).
- [20] T. Sjostrand and M. van Zijl, *Phys. Rev. D* **36**, 2019 (1987).
- [21] X. N. Wang, *Phys. Rev. D* **43**, 104 (1991).
- [22] A. Capella, U. Sukhatme, C. I. Tan, and J. T. Thanh Van, *Phys. Rep.* **236**, 225 (1994).
- [23] A. B. Kaidalov, *Phys. At. Nucl.* **66**, 1994 (2003).
- [24] V. Khachatryan *et al.* (CMS Collaboration), *J. High Energy Phys.* **01** (2011) 079.
- [25] R. Aaij *et al.* (LHCb Collaboration), *Eur. Phys. J. C* **74**, 2888 (2014).
- [26] A. Breakstone *et al.* (Ames-Bologna-CERN-Dortmund-Heidelberg-Warsaw Collaboration), *Phys. Rev. D* **30**, 528 (1984).
- [27] R. P. Feynman, *Phys. Rev. Lett.* **23**, 1415 (1969).